Letter Vol. 41, No. 18 / September 15 2016 / Optics Letters 4383

Optics Letters

Single-step sub-200 fs mid-infrared generation from an optical parametric oscillator synchronously pumped by an erbium fiber laser

Bernd Metzger,[1] Benjamin Pollard,[1] Ingo Rimke,[2] Edlef Büttner,[2] and Markus B. Raschke[1,*]

[1]Department of Physics, Department of Chemistry, and JILA, University of Colorado, 2000 Colorado Ave., Boulder, Colorado 80309, USA
[2]APE Angewandte Physik und Elektronik GmbH, Plauener Str. 163-165, 13053 Berlin, Germany
*Corresponding author: markus.raschke@colorado.edu

Received 1 August 2016; revised 23 August 2016; accepted 24 August 2016; posted 25 August 2016 (Doc. ID 272826); published 15 September 2016

We demonstrate the single-step generation of mid-infrared femtosecond laser pulses in a $AgGaSe_2$ optical parametric oscillator that is synchronously pumped by a 100 MHz repetition rate sub-90 fs erbium fiber laser. The tuning range of the idler beam in principle covers ∼3.5 to 17 μm, only dependent on the choice of cavity and mirror design. As an example, we experimentally demonstrate idler pulse generation from 4.8 to 6.0 μm optimized for selective vibrational resonant molecular spectroscopy. We find an oscillation threshold as low as 150 mW of pump power. At 300 mW pump power and a central wavelength of ∼5.0 μm, we achieve an average infrared power of up to 17.5 mW, with a photon conversion efficiency of ∼18%. A pulse duration of ∼180 fs is determined from a nonlinear cross-correlation with residual pump light. The single-step nonlinear conversion leads to a high power stability with <1% average power drift at <0.5% rms noise over 1 h.

OCIS codes: (190.4970) Parametric oscillators and amplifiers; (300.6340) Spectroscopy, infrared; (320.7090) Ultrafast lasers.

http://dx.doi.org/10.1364/OL.41.004383

Femtosecond mid-infrared (IR) laser pulses, tunable over a broad spectral range, are required in a wide range of applications such as time and frequency domain spectroscopy of molecular vibrations, lattice phonons, and low-energy electronic excitations. For the generation of ultrafast mid-IR laser pulses, high-power visible or near-IR femtosecond pump light is typically converted into the mid-IR by optical parametric oscillators (OPOs) [1–4] or amplifiers [5–7], followed by difference frequency generation (DFG) [8–13] of a combination of pump, signal, and idler beams.

It is, however, highly desirable to reach the mid-IR in a single nonlinear conversion step, to increase the power stability, and to achieve an overall higher nonlinear optical conversion efficiency, while simultaneously reducing cost and experimental complexity.

A major limitation of single-step nonlinear frequency conversion from the visible or near-IR to the mid-IR is the availability of nonlinear optical crystals, which need to fulfill several requirements to be suitable for efficient mid-IR generation. The nonlinear optical materials ought to show appropriate birefringence for phase matching, exhibit a high optical nonlinearity, and need to be transparent at all relevant frequencies, in particular, also at twice the pump frequency to avoid two-photon absorption. However, the range of possible materials is limited for fundamental reasons. Low-frequency IR transmission requires soft phonon modes; yet, the associated soft lattice potentials are quantum-mechanically linked to small bandgap energies. To achieve widely tunable single-step mid-IR generation using 800 or 1064 nm pumping, e.g., lithium-based chalcogenides have been identified as viable candidates [14–17]. Yet, difficulties in crystal growth have remained a limiting factor [16,18]. In addition, for pumping at near-visible frequencies, the necessary increase in bandgap energy is typically connected to a smaller second-order nonlinear optical coefficient [19].

In this Letter, we demonstrate single-step mid-IR generation using longer wavelength pumping in the telecom wavelength range. We synchronously pump an OPO based on silver gallium selenide ($AgGaSe_2$) [20,21], which is widely available with good crystal quality. $AgGaSe_2$ shows a bulk transparency window spanning from 710 nm to 18 μm and, hence, it can be directly pumped above about 1.42 μm [22,23]. Furthermore, due to its wide transparency into the mid-IR, it is a good candidate for broadly tunable mid-IR generation. For example, when pumping $AgGaSe_2$ at the convenience of a typical telecom wavelength of 1.56 μm, which also has the advantage of a reduced group velocity mismatch between the involved pump, signal, and idler frequencies, it is in principle possible to achieve tunability of the idler wavelength from about 3.5–17 μm, as seen in Fig. 1(a). In addition, $AgGaSe_2$ exhibits adequate thermal conductivity of about $\sim 1\ \mathrm{W/(m \cdot K)}$ [24] and a damage threshold greater than $\sim 1\ \mathrm{J/cm^2}$ [25]. Most importantly, it features a high second-order nonlinear optical coefficient d_{eff} of about 34 pm/V compared to other nonlinear optical materials for mid-IR generation [26]. Figure 1(b) shows the calculated near-IR signal

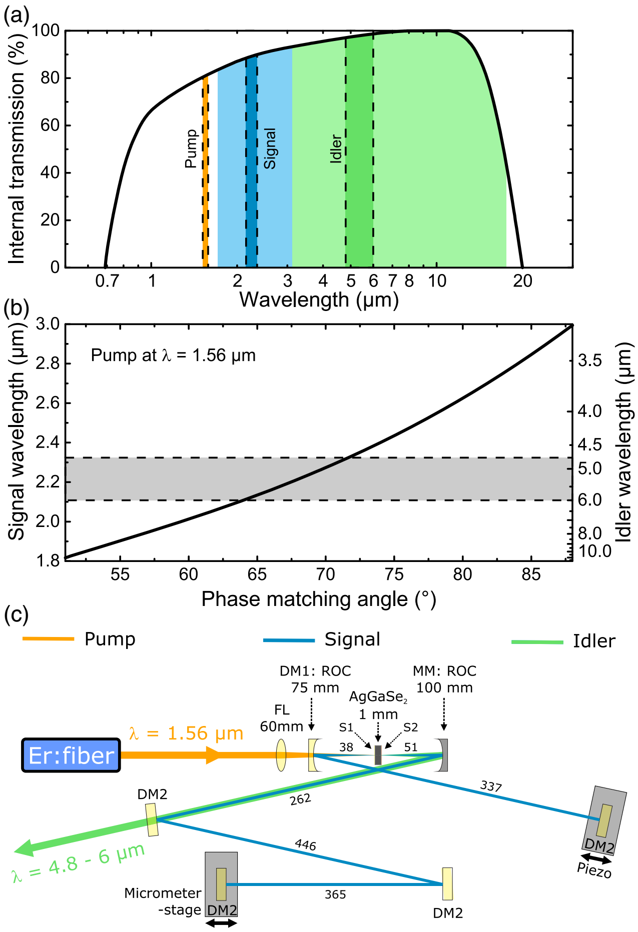

Fig. 1. (a) Schematic bulk transmission spectrum of $AgGaSe_2$ [22]. The light colored areas indicate the full theoretical tuning range. The spectral range exploited in our experiments of the signal and idler wavelengths is shown as the framed regions. (b) Calculated phase-matching angles in $AgGaSe_2$ for type I phase matching [23]. (c) Experimental OPO setup for single-step generation of tunable sub-200 fs mid-IR laser pulses (FL, focusing lens; DM, dichroic mirror; ROC, radius of curvature; MM, metallic mirror; S1 and S2, optical coatings [see text]; black numbers, distances in mm).

and mid-IR idler wavelengths as a function of the phase-matching angle in $AgGaSe_2$ for type I phase matching (pump, e; signal, idler, o) and pumping at 1.56 µm.

To demonstrate the general feasibility of $AgGaSe_2$ as a nonlinear material for single-step OPO mid-IR generation based on telecom wavelength pumping, we aim for an idler tuning range from below 5 up to 6 µm with a corresponding signal wavelength ranging from about 2.1–2.35 µm. This wavelength range has been chosen for applications in molecular and soft-matter vibrational spectroscopy to access resonant frequencies of important functional groups of various molecules, for example carbonyl modes (~1700–2100 cm^{-1}) and protein amide I modes (~1650–1680 cm^{-1}) [27].

Our 1 mm thick $AgGeSe_2$ crystal (Ascut Ltd.) is cut at an angle θ of 70° and is anti-reflection (AR)-coated for the pump (1.56 µm) and the signal (1.9–2.5 µm) on side S1, as well as for the signal (1.9–2.5 µm) and the idler (4–8.5 µm) on side S2; see Fig. 1(c). To pump the $AgGeSe_2$ crystal, we use a compact 100 MHz repetition rate sub-90 fs erbium fiber laser (Menlo Systems, C-fiber high power) with a central wavelength of ~1.56 µm [28–30].

As shown in Fig. 1(c), after passing telescope optics, the pump light is focused into the $AgGaSe_2$ crystal to a beam waist of ~50 µm in diameter. A singly resonant linear OPO cavity has been designed using standard methods of Gaussian beam propagation. In our cavity design, the signal light is not coupled out of the cavity to ensure the highest possible conversion efficiency into the mid-IR idler beam. At the input side of the cavity, we use a dielectric spherical mirror DM1 (LohnStar Optics) with a coating that is AR for the pump wavelength and additionally highly reflective (HR) from 2.09 to 2.34 µm for the signal wavelength. The cavity is folded using several dielectric mirrors DM2, which are HR in the same spectral range as DM1 and AR from 4.6 to 6.0 µm. Thus, the first DM2 mirror after the crystal serves as an idler output coupler. For coarse and fine cavity length adjustment, the two end mirrors of the cavity are mounted onto a micrometer and a Piezo stage, respectively. After the output coupler, we use a germanium filter to separate the mid-IR laser pulses from the residual pump light.

After the alignment of the cavity mirrors and the cavity length, the initial start of OPO oscillation is detected by observing the depleted pump on an InGaAs detector. Subsequently, the alignment of the OPO cavity is optimized by measuring the idler pulses with a mercury cadmium telluride detector. For long-term operation, we also actively stabilize the cavity length to compensate for the small drifts of the repetition rate of the pump laser, as well as the small thermal drifts of the OPO cavity. Therefore, a small fraction of the idler laser pulses measured with a thermal power meter is used as a feedback signal to actively adjust the position of the Piezo end mirror using only a proportional loop algorithm.

To tune the OPO, we employ angle tuning of the $AgGaSe_2$ crystal. Figure 2(a) shows idler spectra measured with a Fourier-transform IR (FTIR, Thermo Nicolet 6700) spectrometer, together with the corresponding average power values (Ophir 3A), for phase-matching angles from about 63 to 73°. At a pump power of 300 mW we achieve a tuning range from about 4.8–6.0 µm with an average output power of up to 17.5 mW, which corresponds to a photon conversion efficiency of 18%. Furthermore, the spectra exhibit a full-width half-maximum bandwidth, ranging from about 300–340 nm. The OPO itself is dry air purged; however, the laser pulses had to travel a distance of about 2 m outside the enclosure to the FTIR spectrometer, resulting in atmospheric absorption lines. The tuning range is predominantly limited by the reflectivity of the cavity mirrors, as indicated by the gray area in Fig. 1(b). Furthermore, the peak in the output power at ~5 µm wavelength can predominantly be attributed to the combined performance of the AR- and HR-coatings at the signal wavelength of the crystal and the cavity mirrors, respectively.

To characterize the mid-IR pulse duration, we first characterized the residual pump laser pulses at 1.56 µm using interferometric frequency-resolved optical gating [31]. Subsequently, we performed a cross-correlation between the idler laser pulses tuned to ~5 µm and the residual pump laser light. For that purpose, the germanium filter was removed and reconfigured as a beam splitter in a Michelson interferometer. After the Michelson interferometer, the collinear residual pump and idler laser pulses

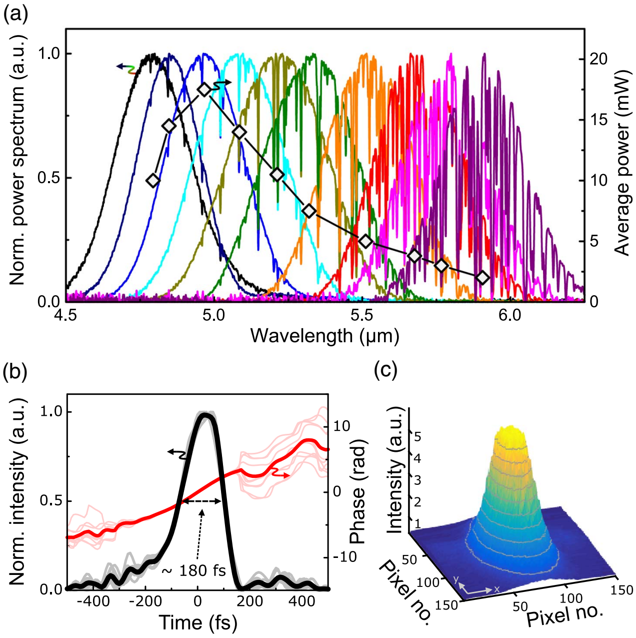

Fig. 2. (a) Measured normalized OPO idler spectra and corresponding average powers (diamonds) when angle tuning the $AgGaSe_2$ crystal. (b) Retrieved temporal electric field intensity and phase of the idler laser pulses at a wavelength of ∼5.0 μm using a DFG cross-correlation with the residual pump laser pulses. (The shaded curves correspond to the intensity and phase of 10 subsequent iterations of the retrieval algorithm; the solid lines show the average result.) (c) Measured beam profile of the idler laser pulses.

were focused into an identically cut $AgGaSe_2$ crystal, and the resulting DFG cross-correlation signal was measured in a delay and frequency-resolved fashion. From the characterization of the residual pump laser pulses and the measured DFG cross-correlation, the electric field transient of the mid-IR laser pulses can be determined using an appropriate cross-correlation FROG retrieval algorithm [32,33]. The retrieved temporal electric field intensity and phase are shown in Fig. 2(b), corresponding to a pulse duration of ∼180 fs (FWHM). Since the Fourier limit of the idler pulses is ∼100 fs the mid-IR laser pulses exhibit only small dispersion, which we predominantly attribute to the dispersion of the pump laser pulses of the fiber laser that are not Fourier limited and, partially, to the dispersion of the different optical elements in the setup.

Figure 2(c) shows the spatial beam profile of the idler pulses measured with an IR-camera (DataRay, WinCamD-FIR2-16), which exhibits a Gaussian shape to a good approximation with only small ellipticity. From the measurement of the caustic of the idler beam, we determine an M^2 factor of <1.1 and <1.3 in the horizontal and vertical direction, respectively.

The threshold behavior of the OPO can be seen in Fig. 3, which shows the idler average output power and the photon conversion efficiency at an idler wavelength of ∼5.0 μm as a function of the average input power. We find an oscillation threshold of only ∼150 mW of pump power.

To demonstrate the long-term stability of the setup, we concurrently monitored the idler average power and the idler power spectrum over 1 h, while simultaneously actively stabilizing the cavity length. The result of a typical

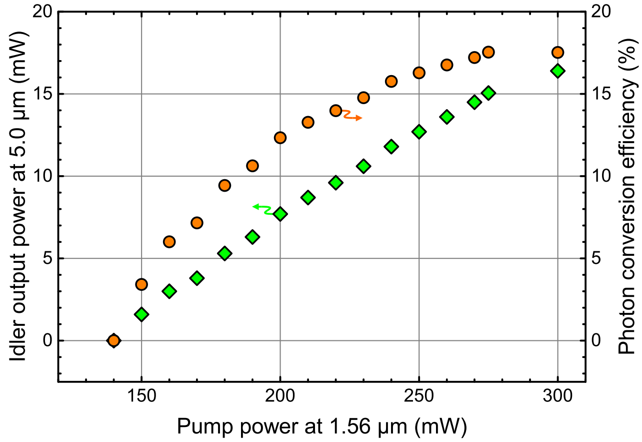

Fig. 3. Idler average output power at a wavelength of ∼5.0 μm and the photon conversion efficiency as a function of the average pump power at a center wavelength of ∼1.56 μm.

measurement is shown in Fig. 4. We find a high power stability with <1% average power drift, power fluctuations <0.5% rms, and a standard deviation of the central wavelength of less than 2.5 nm over 1 h. This illustrates the stability advantage of a single-step nonlinear conversion for mid-IR generation, when compared to typical power stabilities of ultrafast mid-IR laser sources that rely on cascaded nonlinear optical processes.

The tunability of our OPO can be extended by the use of mirror coatings optimized for an extended wavelength range. To achieve an optimal performance of the OPO in certain wavelength regimes, it also might be necessary to select a different cutting angle of the $AgGaSe_2$ crystal, since a tilt angle of the crystal required for phase matching that is too large introduces additional reflection losses at the crystal surface. Furthermore, an increase in the spectral bandwidth and reduced pulse durations should be possible using thinner $AgGaSe_2$ crystals, in

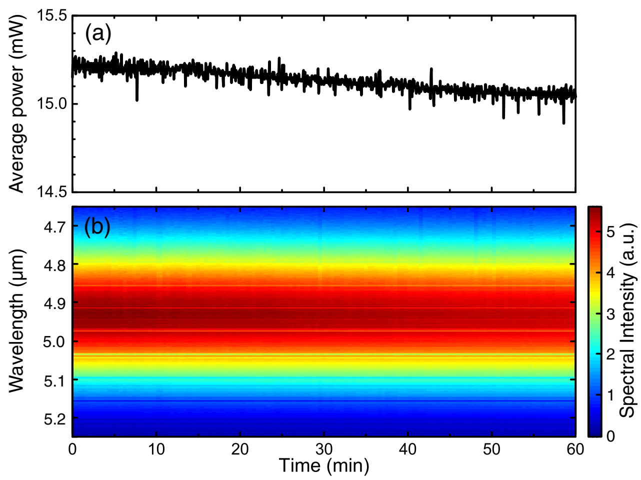

Fig. 4. (a) Average power stability and (b) spectral stability measured over 1 h. We find power stability with <1% average power drift and power fluctuations <0.5% rms. In the case of the average power, a data point was recorded every 2 s with a thermal power meter. For the spectral stability, a spectrum was measured every 30 s using an FTIR spectrometer.

combination with Fourier-limited pump laser pulses, though a thinner crystal might reduce the overall conversion efficiency.

In conclusion, we demonstrated the single-step generation of femtosecond mid-IR laser pulses using a highly compact optical parametric oscillator based on silver gallium selenide ($AgGaSe_2$). As a pump laser source, we employed a sub-90 fs erbium fiber laser at a wavelength of ~1.56 μm. The idler laser pulses of the OPO were tuned from about 4.8–6.0 μm, with a pulse duration of about ~180 fs and an average power of up to 17.5 mW. Compared to cascaded DFG, single-step mid-IR generation allows for much higher conversion efficiencies, in our case, as high as 18%, as opposed to the overall photon conversion efficiencies of two-step mid-IR generation of typically only a few percent [9,10,12]. The single-step approach also enables a highly stable operation with power fluctuations smaller than 0.5% rms over an hour and a very cost-efficient setup. In the future, this approach will also benefit from further developments in erbium laser technology, possibly providing higher pulse energies, as required for nonlinear mid-IR spectroscopies.

Funding. National Science Foundation (NSF) (CHE 1531996).

Acknowledgment. The authors thank Robin Hegenbarth, Scott Diddams, Stefan Marzenell, Thomas Schibli, and Jun Ye for valuable discussions and advice.

REFERENCES

1. J. Hebling, R. Szipöcs, E. J. Mayer, and J. Kuhl, Opt. Lett. **20**, 919 (1995).
2. T. Südmeyer, E. Innerhofer, F. Brunner, R. Paschotta, T. Usami, H. Ito, S. Kurimura, K. Kitamura, D. C. Hanna, and U. Keller, Opt. Lett. **29**, 1111 (2004).
3. D. Reid, J. Sun, T. Lamour, and T. Ferreiro, Laser Phys. Lett. **8**, 8 (2011).
4. T. Lang, T. Binhammer, S. Rausch, G. Palmer, M. Emons, M. Schultze, A. Harth, and U. Morgner, Opt. Express **20**, 912 (2012).
5. R. A. Kaindl, M. Wurm, K. Reimann, P. Hamm, A. M. Weiner, and M. Woerner, J. Opt. Soc. Am. B **17**, 2086 (2000).
6. G. Cerullo and S. De Silvestri, Rev. Sci. Instrum. **74**, 1 (2003).
7. M. Marangoni, R. Osellame, R. Ramponi, G. Cerullo, A. Steinmann, and U. Morgner, Opt. Lett. **32**, 1489 (2007).
8. F. Seifert, V. Petrov, and M. Woerner, Opt. Lett. **19**, 2009 (1994).
9. S. Ehret and H. Schneider, Appl. Phys. B **66**, 27 (1998).
10. R. Hegenbarth, A. Steinmann, S. Sarkisov, and H. Giessen, Opt. Lett. **37**, 3513 (2012).
11. M. Beutler, I. Rimke, E. Büttner, V. Petrov, and L. Isaenko, Opt. Mater. Express **3**, 1834 (2013).
12. M. Beutler, I. Rimke, E. Büttner, P. Farinello, A. Agnesi, V. Badikov, D. Badikov, and V. Petrov, Opt. Express **23**, 2730 (2015).
13. I. Pupeza, D. Sánchez, J. Zhang, N. Lilienfein, M. Seidel, N. Karpowicz, T. Paasch-Colberg, I. Znakovskaya, M. Pescher, W. Schweinberger, V. Pervak, E. Fill, O. Pronin, Z. Wei, F. Krausz, A. Apolonski, and J. Biegert, Nat. Photonics **9**, 721 (2015).
14. F. Rotermund, V. Petrov, F. Noack, L. Isaenko, A. Yelisseyev, and S. Lobanov, Appl. Phys. Lett. **78**, 2623 (2001).
15. V. Petrov, V. Badikov, V. Panyutin, G. Shevyrdyaeva, S. Sheina, and F. Rotermund, Opt. Commun. **235**, 219 (2004).
16. L. Isaenko, A. Yelisseyev, S. Lobanov, P. Krinitsin, V. Petrov, and J.-J. Zondy, J. Non-Cryst. Solids **352**, 2439 (2006).
17. G. Marchev, A. Tyazhev, V. Vedenyapin, D. Kolker, A. Yelisseyev, S. Lobanov, L. Isaenko, J.-J. Zondy, and V. Petrov, Opt. Express **17**, 13441 (2009).
18. M. Zhou, L. Kang, J. Yao, Z. Lin, Y. Wu, and C. Chen, Inorg. Chem. **55**, 3724 (2016).
19. L. Kang, M. Zhou, J. Yao, Z. Lin, Y. Wu, and C. Chen, J. Am. Chem. Soc. **137**, 13049 (2015).
20. S. Marzenell, R. Beigang, and R. Wallenstein, Appl. Phys. B **69**, 423 (1999).
21. R. Hegenbarth, A. Steinmann, S. Mastel, S. Amarie, A. J. Huber, R. Hillenbrand, S. Y. Sarkisov, and H. Giessen, J. Opt. **16**, 094003 (2014).
22. H. Kildal and J. Mikkelsen, Opt. Commun. **9**, 315 (1973).
23. A. V. Smith, *Crystal Nonlinear Optics: With SNLO Examples* (AS-Photonics, 2016).
24. N. P. Barnes and J. A. Williams-Byrd, J. Opt. Soc. Am. B **12**, 124 (1995).
25. B. C. Ziegler and K. L. Schepler, Appl. Opt. **30**, 5077 (1991).
26. R. W. Boyd, *Nonlinear Optics*, 3rd ed. (Academic, 2008).
27. E. A. Muller, B. Pollard, and M. B. Raschke, J. Phys. Chem. Lett. **6**, 1275 (2015).
28. P. E. Britton, H. L. Offerhaus, D. J. Richardson, P. G. R. Smith, G. W. Ross, and D. C. Hanna, Opt. Lett. **24**, 975 (1999).
29. S. Desmoulins and F. D. Teodoro, Opt. Lett. **32**, 56 (2007).
30. M. W. Haakestad, H. Fonnum, G. Arisholm, E. Lippert, and K. Stenersen, Opt. Express **18**, 25379 (2010).
31. G. Stibenz and G. Steinmeyer, Opt. Express **13**, 2617 (2005).
32. S. Linden, H. Giessen, and J. Kuhl, Phys. Status Solidi B **206**, 119 (1998).
33. R. Trebino, *Frequency-Resolved Optical Gating: The Measurement of Ultrashort Laser Pulses* (Springer, 2000).